Nuclear Instruments and Methods in Physics Research A324 (1993) 113–126
North-Holland

NUCLEAR
INSTRUMENTS
& METHODS
IN PHYSICS
RESEARCH
Section A

Measurement of electron drift parameters for helium and CF_4-based gases *

J. Va'vra
Stanford Linear Accelerator Center, Stanford University, Stanford, CA 94309, USA

P. Coyle [1]
Santa Cruz Institute for Particle Physics, University of California, Santa Cruz, CA 95064, USA

J. Kadyk and J. Wise
Lawrence Berkeley Laboratory, University of California, Berkeley, CA 94720, USA

Received 3 June 1992

We have studied various helium and CF_4-based gas mixtures, which may have important applications for the SSC, Phi, Tau-charm, and B factories. We present an integrated set of measurements, which includes the drift velocity, longitudinal single electron diffusion, characteristic electron energy, single electron pulse height spectra, operating wire gain, relative cathodic breakdowns in different gases, effect of water addition on the drift parameters, impurity problems in the CF_4-based gases, diffusion near the wire and wire aging. The data are compared to predictions based on electron transport theories.

1. Introduction

The need to reduce event occupancy in straw tube detectors at the Superconducting Super Collider (SSC), has led to considerable interest in radiation hard, fast gases based on CF_4. In addition, the need for improved momentum resolution in the central tracking chambers of future Phi, Tau-charm or B factories has lead to the study of low mass gases with reduced multiple scattering based on helium.

We are primarily interested in parameters such as drift velocity and single electron longitudinal diffusion. These quantities can be used, for instance in drift chamber simulation programs to predict resolution for a particular geometry, or as input to obtain the cross sections for an electron transport theory, or simply to check results of the theoretical predictions of existing electron transport computer codes. In this paper we concentrate on the latter point. It should be noted that existing codes either do not contain parameters of gases such as CF_4 or dimethyl ether (DME) or have them parametrized poorly (DME gas was considered as a quencher).

In addition, we are also interested in the single electron pulse height spectra, the characteristic electron energy and cathodic breakdowns, since these tend to reveal underlying problems related, for instance, to an incorrect operating point or an insufficient amount of quencher in the mixture.

We found that CF_4-based gases often have impurities which can attach the drifting electrons, resulting in loss of signal. Therefore, it was important to study how to purify such gases and to determine whether their wire aging was correlated with these impurities. We have also performed wire aging studies on two types of He-based gases, one where the electrons heat up (i.e., become more energetic) and one where they are relatively cool (i.e., are close to thermal energies).

Many studies have found it necessary to add water to the gas mixtures in order to prevent or limit the wire aging [1,2]. Therefore we have studied the effect of water addition on the drift velocity and longitudinal diffusion.

It has been suggested [3] that electron diffusion near the anode wire is an important contribution to the tracking resolution. Since electrons in the He gas mixtures tend to heat readily in high electric field, we have decided to study this question in such gases.

* Work supported by Department of Energy contract DE-AC03-76SF00515.

1 Present address: Centre de Physique des Particules, Faculté des Sciences de Luminy CNRS, 13288 Marseille, France.

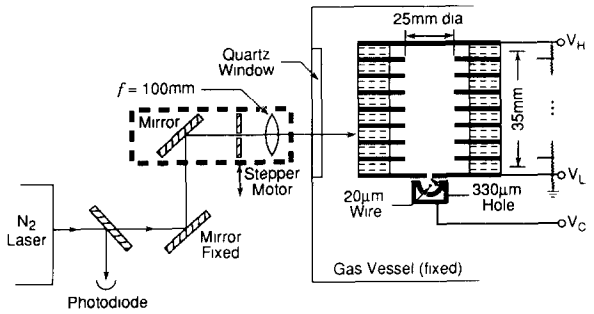

Fig. 1. Experimental setup of this paper.

In summary, we present an integrated look at the He and CF_4 gas mixtures, which includes measurements of drift velocity, longitudinal single electron diffusion, characteristic electron energy as a function of electric field, single electron pulse height spectra, operating gain, relative cathodic breakdowns in different gases, effect of water addition on the drift parameters, impurity problems in the CF_4-based gases and diffusion near the wire in He-based gases. We also present some results on wire aging. The results presented for the CF_4-based gases are a continuation of a previous R&D program related to straw tube detectors [2].

2. Description of experimental apparatus

The drift velocity, longitudinal diffusion and pulse height spectra refer to single electrons in this paper. Measurements were made using the experimental setup shown in fig. 1. A N_2-laser [4] beam was reflected by two mirrors into a stationary drift cell through a quartz lens of 10 cm focal length. The focal point was in the middle of active drift volume. The position of the second mirror could be controlled using a stepper motor [5] allowing the laser beam position to be moved in precisely known steps. A portion of the laser beam was reflected to a photodiode [6] which was used as a reference start for the timing measurements. To ensure that we were dealing with single electrons the probability of having an event per laser shot was set to less than 10% by attenuating the laser beam.

The drift cell was made of two sections: a drift region made of equally spaced stainless steel rings and a gain region containing a 20 μm gold-plated anode wire surrounded by a nickel plated cathode [7]. The gain and the drift regions were separated by a stainless steel foil which had a 330 μm diameter hole allowing electrons to enter the gain region. The purpose of this restriction was to ensure that the timing spread due to the collection geometry would not affect the timing spread due to diffusion. Moreover, we could change the drift field without affecting the gain and vice versa.

When measuring the longitudinal and transverse diffusion one cannot measure only one and switch off the other, and transverse diffusion will affect the measurement of longitudinal diffusion. Our restrictive geometry is less sensitive to these effects, because it reduces tails of charge collection. The total length of the drift region was about 35 mm. The spacers between the stainless steel rings had a small opening for the laser beam allowing a typical step of 5 mm between two laser positions. The closest anode wire to cathode distance was about 1.4 mm, and the anode wire to the hole distance was about 2.85 mm.

The drift field was defined by the potentials V_L and V_H (fig. 1). The resistor chain provided voltages to the individual stainless steel rings. The maximum drift field was typically 2 kV/cm/atm and was limited by either the 10 kV power supply limit or a cathodic breakdown in the drift structure. To minimize the effect of the resistor voltage coefficient, we used five resistors in series between each stainless steel ring (the voltage drop per resistor is smaller). The value of each resistor was 10 MΩ. The groups of five resistors were selected empirically at full operating voltage to be accurate to 0.2% of each other.

The wire gain was controlled by the potentials V_C and V_L. Typically, the gain was kept fixed and the drift field varied by changing the V_H voltage in small steps. The $V_C - V_L$ voltage difference was kept constant at 300 V.

We have used an amplifier from the CRID detector of the SLD experiment [8] to detect the single electron avalanches. The amplifier output was split using a LRS-612 post-amplifier and the two outputs were discriminated at two different threshold levels. Both signals were then digitized separately in a LRS TDC-2228. This procedure allowed an off-line correction for time slewing to be applied as illustrated in fig. 2a. Fig. 2b shows that the t_0 distribution is Gaussian even though the distribution of the t_1 and t_2 variables tend to have tails. This technique works well for our application where we deal with single electrons and the normalized pulse shape is always the same. It does not work well, generally, for drift chambers where there are many electrons per pulse and the avalanche fluctuations cause a randomness in the pulse shapes. The t_0 distribution was fitted to extract a mean and sigma for each laser step. To cover the full range of drift velocities and diffusion values we used two different TDCs and selected 2.5, 1.0, 0.5 and 0.25 ns/TDC bin. It was important to calibrate the TDC with delay lines to avoid systematic errors. The drift velocity was calculated using a linear fit to the mean values as a function of distance, the diffusion using a linear fit to the σ^2 values as a function of distance.

We measured the single electron pulse height spectra using a LRS QVT-3001 operated in the q-mode

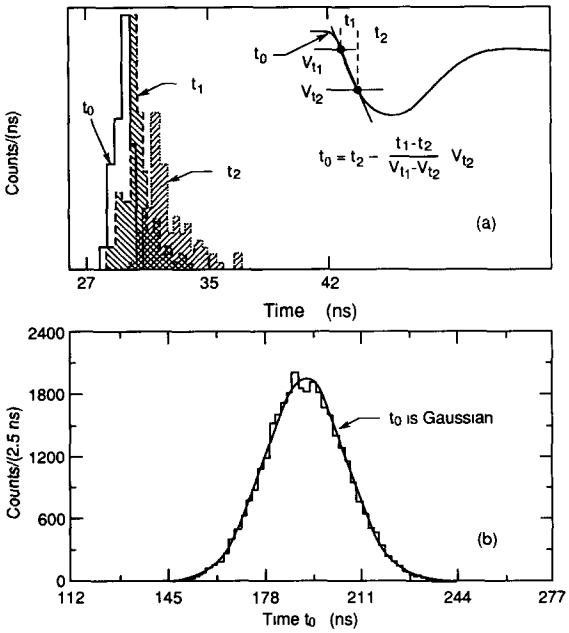

Fig. 2. (a) Typical timing distributions obtained for three different timing methods t_0, t_1 and t_2. (b) Curve is a Gaussian fit to data using t_0 timing.

with an internal 450 ns gate width. In order to estimate the wire gain we have calibrated the qVt spectrum by injecting charge into the amplifier input. We fitted the single electron pulse height spectra with a Polya function and estimated the mean "visible" gain from the fit. We also applied a cut on small pulses near the pedestal typically below 2–4 fC, to avoid a region near the threshold of the internal gating circuit. This procedure was checked periodically by either varying the cut or by switching to an external gating method. A correction to get the total wire gain was calculated using a knowledge of the qVt gate width, mobility of positive ions [9] and known time development of the charge, assuming for simplicity a cylindrical geometry [10]. The correction factor was found to be typically about 1.6.

The whole process was controlled by a Macintosh IIcx with a Bergoz MAC-CC controller coupled to CAMAC and GPIB interfaces. The GPIB interface controlled a Keithley digital multi-meter no. 196 which monitored various analog voltages and resistances [11]. The system measured gas temperature [12] and barometric pressure [13] to allow a calculation of E/p and correct it to 298°C and 1 atm = 1013.6 mbar. In addition we monitored oxygen [14] and water concentration [15]. The software was based on MAC-UA1 software [16], and included improvements to allow on-line fitting to linear, Gaussian and Polya functions. The measurement operation was completely under computer control, including the laser beam positioning, voltage control of Bertan power supplies, etc. The typical event logging rate was 20 Hz.

Generally we obtained bottles of premixed gas, but in the case of helium/DME, the mixing was performed using two mass flow controllers [17]. It was essential to calibrate the mass flow controllers using a bubble flow meter. We used an Oxisorb filter and a 13X molecular sieve during all measurements to remove the oxygen and water. When using these filters, the oxygen and water concentrations were typically below 5 and 10 ppm, respectively, monitored downstream of the drift chamber. For some special tests we added small amounts of water to the gas using a permeation tube technique [18] in which the water permeates, at a temperature-dependent rate, through the Teflon walls of the tube into the surrounding gas flow (this process could be accelerated by heating). We could add up to about 1000 ppm of water to the gas with this technique.

The errors plotted on the drift velocity and the longitudinal diffusion graphs are statistical only, and are determined to be less than 1% and 3–10%, respectively. The systematic errors are estimated to be at a level of about 3%. These errors are related to the gas ratios, TDC calibration, geometrical effects, etc.

3. Results

3.1. Comparison with existing data and models

The first task was to verify that the apparatus reproduced existing measurements. Fig. 3 shows such comparison for a 50% Ar + 50% C_2H_6 gas. One can see that our drift velocity data agree with other data [19] shown on fig. 3a. Fig. 3b shows that our longitudinal diffusion data are half way between the data of Wong et al. [20] and Fehlmann [21], consistent with the point of Jean-Marie et al. [22], and are lower than the data of Piuz [23]. The solid curve is a $1/\sqrt{E}$ fit to our data (the first eight points used to constrain the fit). The $1/\sqrt{E}$ is expected for thermal electrons (with energy = kT, where k is the Boltzmann constant, T is the absolute temperature). To illustrate the results of calculations based on modern electron transport theory, we show three examples: a) the dot–dashed curve in fig. 3b, which is the second-order solution to Boltzmann equation due to Biagi [24]; b) the dashed curve which is the first-order solution to Boltzmann equation based on a calculation of Fraser and Mathieson [27]; c) and the dotted curve which is a calculation using the computer program WIRCHA [28]. The best agreement with our data is given by the Biagi's calculation using his program MAGBOLTZ. This program follows an algorithm given by Huxley and Crompton [29], with the

addition of ionization and attachment collision cross sections. Our data were not part of the electron-gas cross section fitting. We will return to discuss model comparisons in the sections below.

3.2. Drift velocity and longitudinal diffusion in CF_4-based gases

We found that many of our CF_4-based gas mixtures [30] were significantly contaminated. The result of this contamination was that a typical electron drift distance was less than about a centimeter, preventing any useful measurements. None of the usual cleaning techniques involving Oxisorb or molecular sieve helped. Finally, we found a reliable way to clean these mixtures, using a Nanochem filter [31] selected to remove halogen impurities such as Freon-11. None of the He-based mixtures showed such problems. DME can also have contamination problems; however, in our case, we used a clean DME gas from Majewski [32].

CF_4 can be operated without any quencher provided that one keeps the wire gain below about 10^6 operating in the single electron mode (section 3.6). However, it is safer to add a quenching gas to CF_4 in experimental applications. Results for CH_4, iC_4H_{10} and DME quenchers are shown in fig. 4. One can see that even a

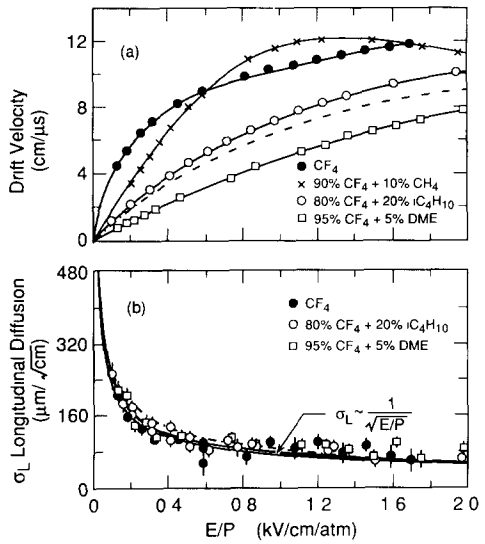

Fig. 4. (a) Our measurement of electron drift velocity in the CF_4-based gases. The solid curves are to guide the eye and the dot-dash curve is a calculation of Biagi [24] for 80% CF_4 + 20% iC_4H_{10} gas. (b) Our measurement of single electron longitudinal diffusion in the CF_4-based gases. The solid curves are $1/\sqrt{E}$ (all points used in the fit) and the dot-dash curve is a calculation of Biagi [24] for 80% CF_4 + 20% iC_4H_{10} gas.

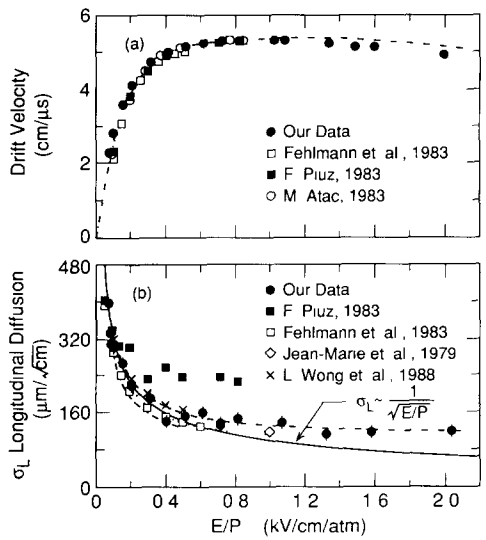

Fig. 3. (a) Comparison of our 50% Ar + 50% C_2H_6 electron drift velocity with other data. The dot-dash curve is a calculation of Biagi [24]. (b) Comparison of our 50% Ar + 50% C_2H_6 single electron longitudinal diffusion with other data. The solid curve is the $1/\sqrt{E}$ fit to our data (the first eight points used to constrain the fit); the other curves are not fit to our data, but are independent predictions: the dot-dash curve is a calculation of Biagi [24], dashed curve is the calculation of Fraser and Mathieson [27], and dotted curve is the prediction of the WIRCHA program [28].

small admixture of DME (5%) reduces the drift velocity considerably. Fig. 5a shows that our CF_4 drift velocity data agree well with results of Schmidt [33], but not as well with results of Christophorou [34] and Hunter [35]. At higher electric fields the discrepancy among published data is larger, as can be seen in fig. 5b, which shows our data along with data of Hunter et al. [35] and Naidu and Prasad [36]. Because of these discrepancies, there is some uncertainty in extracting reliable CF_4 electron scattering cross sections [25]. Consequently, the present version of the CF_4 parametrization in the Biagi code [24,26] does not give very good agreement with our drift velocity data for 80% CF_4 + 20% iC_4H_{10} gas mixture (fig. 4a). Again, one should point out that our data were not used in the calculation to obtain this curve. We hope that the addition of our data into the electron-gas cross section fit might help to resolve this problem, at least in the lower electric field region. Other available computer programs do not have the CF_4 molecule parametrized.

Water has been found to prevent or at least impede wire aging in the straw tubes [1,2]. Therefore it was of some interest to measure the effect of water addition on the drift parameters for a potential straw tube gas candidate. Although we do not see a noticeable effect on the longitudinal diffusion, we do see an effect on the drift velocity. For instance, the drift velocity changes by about 6.3% per 1000 ppm water addition at a drift

field of 1.5 kV/cm/atm in 80% CF_4 + 20% iC_4H_{10} gas (fig. 6a). However, one should remember that this change depends how close we are to the drift velocity plateau, as can be seen in the case of 50% Ar + 50% C_2H_6 (fig. 6b). The longitudinal diffusion is relatively insensitive to the water addition as can be seen in fig. 6c.

3.3. Drift velocity and longitudinal diffusion in He-based gases

Generally the He-based gases have quite low drift velocities. The single electron diffusion begins to be quite acceptable if the amount of a quencher approaches about 15–20% [37]. We have chosen several He-based gas mixtures covering both the less quenched and better quenched gases. Fig. 7 shows our results with 95% He + 5% C_2H_6 and 50% He + 50% C_2H_6. The former gas has been used in the parallel plate amplification chambers [38]. One can see an excellent agreement between our data and the calculations of Biagi [24,26]. The agreement with the program WIRCHA [28] is poor. Fig. 8 shows our data for 93% He + 7% C_3H_8. This gas has been used in the PLUTO drift chamber in a special test run [39]. The data departs from the $1/\sqrt{E}$ behavior which means that the electrons depart from thermal behavior. One can see an excellent agreement with Biagi's calculation. Fig. 9 shows our data for 78% He + 15% CO_2 + 7% iC_4H_{10}. Again, there is a clear indication that the gas is not thermal. There is reasonable agreement with both the

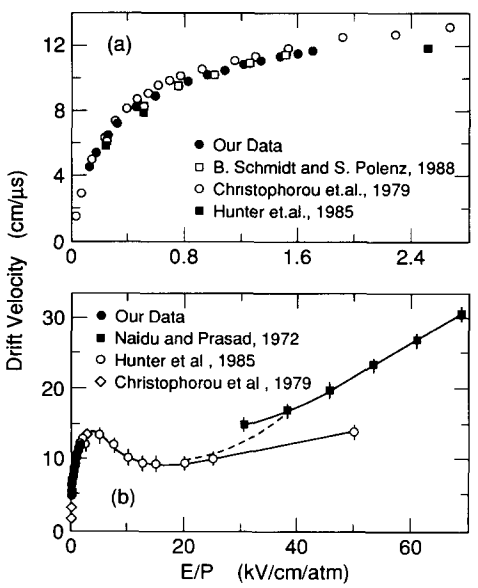

Fig. 5. (a) Comparison of our CF_4 electron drift velocity with other data. (b) Comparison of our CF_4 electron drift velocity with other data at much higher drift field.

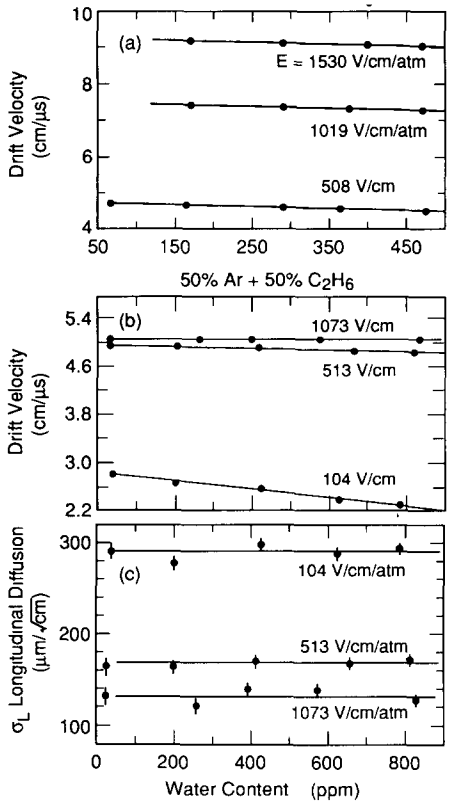

Fig. 6. (a) Our measurement of the drift velocity in 80% CF_4 + 20% iC_4H_{10} as a function of water content. (b) Our measurement of the drift velocity in 50% Ar + 50% C_2H_6 as a function of water content. (c) Our measurement of the longitudinal diffusion in 50% Ar + 50% C_2H_6 as a function of water content.

Biagi calculation and the WIRCHA program. The overall conclusion is that for He-based gases with standard quenchers, the Biagi code is reliable and there doesn't seem to be a further need to measure more such gases in our apparatus.

Fig. 10 shows our data for He/DME mixtures. One can see that the drift velocity agrees only to within about 6–7% and the longitudinal diffusion disagrees even more. Our data were not used in the electron-gas cross section fitting. To help constrain the DME electron-gas cross section in future calculations, we have also measured the DME alone (fig. 11). The MAGBOLTZ program predictions agree with our data to about 5%. For comparison we show also the data of Basile et al. [40] and Cottrell et al. [41]. The Cottrell data were part of the cross section determination.

The maximum drift E/p in figs. 7–11 varies from gas to gas and is limited in our apparatus by cathodic breakdowns (section 3.5). One needs a surprising amount of DME quencher (about 15–20%) to get both

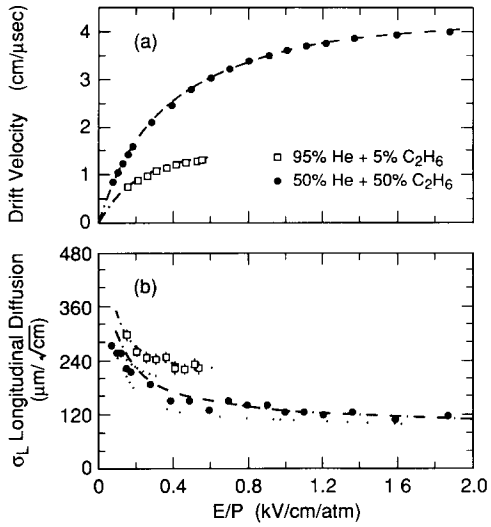

Fig. 7. (a) Our measurement of the electron drift velocity in the 95% He + 5% C_2H_6 and 50% He + 50% C_2H_6 gases. The dot–dash curve is a calculation of Biagi [24]. (b) Our measurement of the single electron longitudinal diffusion in the 95% He + 5% C_2H_6 and 50% He + 50% C_2H_6 gases. The dot–dash curves are calculations of Biagi [24] and the dotted curves are predictions of the WIRCHA program [28].

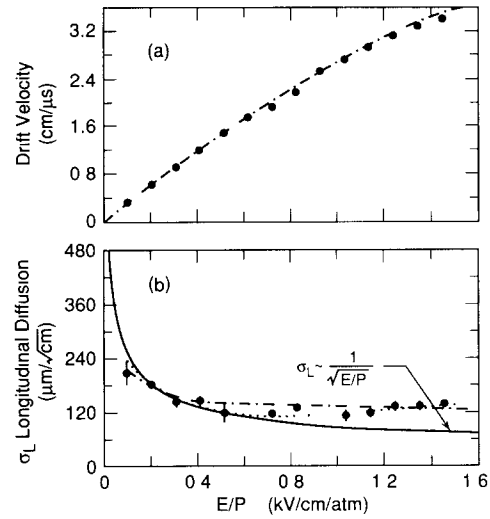

Fig. 9. (a) Our measurement of the electron drift velocity in the 78% He + 15% CO_2 + 7% iC_4H_{10} gas. The dot–dash curve is a calculation of Biagi [24]. (b) Our measurement of the single electron longitudinal diffusion in the 78% He + 15% CO_2 + 7% iC_4H_{10} gas. The dot–dash curve is a calculation of Biagi [24], the dotted curve is prediction of the WIRCHA program [28] and the solid curve is a $1/\sqrt{E}$ fit to our data (the first 4 points used to contrain the fit).

low diffusion and eliminate the problems of cathodic breakdowns. Even so, such DME gas mixtures are not as effective in preventing breakdown as, for example, 78% He + 15% CO_2 + 7% iC_4H_{10} (see table 1 for the breakdown limits). This gas was also studied in a large tracking chamber by a group using an old Mark II

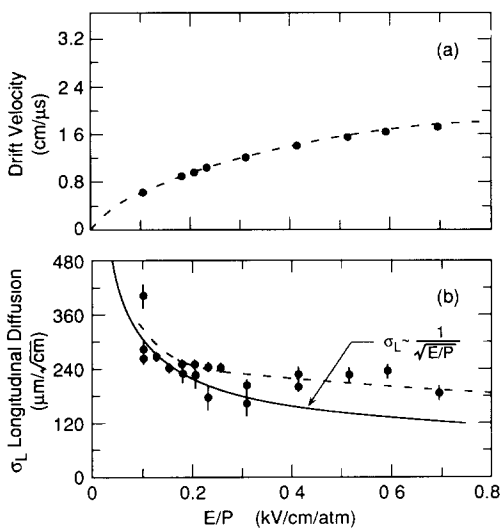

Fig. 8 (a) Our measurement of the electron drift velocity in the 93% He + 7% C_3H_8 gas. The dot–dash curve is a calculation of Biagi [24]. (b) Our measurement of the single electron longitudinal diffusion in the 93% He + 7% C_3H_8 gas. The solid curve is a $1/\sqrt{E}$ fit to black circles (the first nine points used to contrain the fit) and the dot–dash curve is a calculation of Biagi [24].

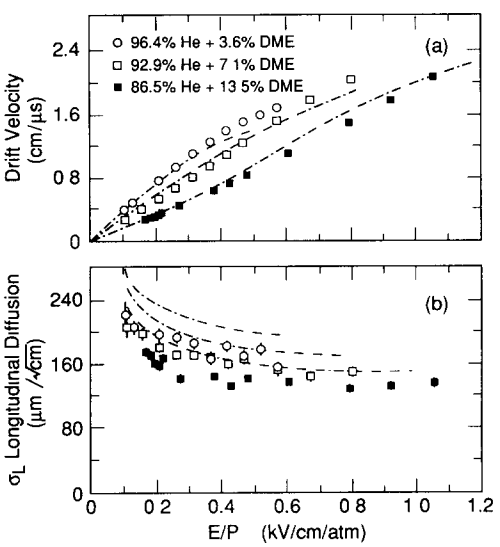

Fig. 10. (a) Our measurement of the electron drift velocity in the He + DME gases. The dot–dash curves are calculations of Biagi [24]. (b) Our measurement of the single electron longitudinal diffusion in the He + DME gases. The dot–dash curves are calculations of Biagi [24].

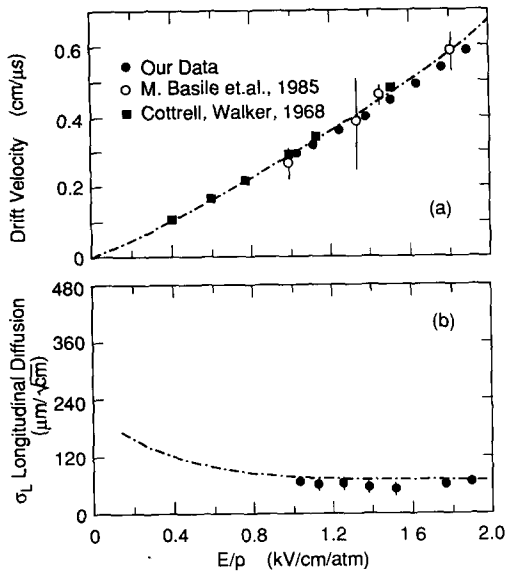

Fig. 11. (a) Our measurement of the electron drift velocity in the DME gas. The dot–dash curve is calculation of Biagi [24]. (b) Our measurement of the single electron longitudinal diffusion in the DME gas. The dot–dash curve is calculation of Biagi [24].

prototype at SLAC [42]. Recently, other groups have also performed studies with He-based gases [37,43].

3.4. Characteristic electron energy

The characteristic electron energy [44] is a useful quantity for estimating how much a drifting electron heats up. The quantity is defined as follows:

$$\epsilon_{L,T} = \frac{eD_{L,T}}{\mu} = \frac{eD_{L,T}E}{\nu} \geq kT \cong 0.025\ [\mathrm{eV}], \qquad (1)$$

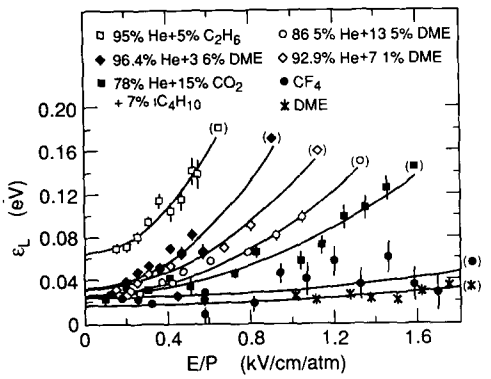

Fig. 12. Our measurement of the characteristic longitudinal energy in various gases. Curves are quadratic fits (table 1).

where $D_{L,T}$ = diffusion constant (longitudinal, transverse), μ = electron mobility, ν = electron velocity, k = Bolzmann constant, E = electric field.

Fig. 12 shows the longitudinal characteristic energy as derived from our measurements of the longitudinal single electron diffusion. One clearly sees that He-based gases with low amount of a quencher heat up very quickly even at very low values of E/p. The CF_4-based and DME gases are near thermal up to 2 kV/cm/atm (see figs. 4b and 12). Table 1 shows results of fits of a quadratic function to our measurements of the longitudinal characteristic energy.

3.5. Cathodic breakdowns

This measurement was done by keeping the V_C and V_L voltages constant and varying the V_H voltage, thus keeping the wire gain constant and varying the drift field. At large enough drift field, the V_H power supply would trip off. The trip off voltage was gas dependent

Table 1
Fit to characteristic energy ϵ_L and maximum drift field achieved before breakdown

Gas	$\epsilon_L = a + b(E/p)^2$		Max E_{drift} [kV/cm/atm]
	a	b	
50% Ar + 50% C_2H_6	0.045 ± 0.0008	0.032 ± 0.003	> 2.0
95% CF_4 + 5% DME	0.028 ± 0.0014	0.012 ± 0.002	> 2.0
80% CF_4 + 20% C_4H_{10}	0.029 ± 0.002	0.004 ± 0.002	> 2.0
90% CF_4 + 10% CH_4	0.049 ± 0.0009	0.013 ± 0.003	> 2.0
100% DME	0.017 ± 0.003	0.0053 ± 0.0012	> 2.0
50% He + 50% C_2H_6	0.034 ± 0.0003	0.044 ± 0.0015	> 2.0
100% CF_4	0.024 ± 0.0008	0.0072 ± 0.003	1.7
78% He + 15% CO_2 + 7% C_4H_{10}	0.026 ± 0.0004	0.044 ± 0.002	1.45
86.5% He + 13.5% DME	0.024 ± 0.0005	0.075 ± 0.003	1.05
92.9% He + 7.1% DME	0.030 ± 0.0007	0.117 ± 0.005	0.8
93% He + 7% C_3H_8-	0.041 ± 0.001	0.269 ± 0.018	0.7
96.4% He + 3.6% DME	0.028 ± 0.001	0.195 ± 0.011	0.58
95% He + 5% C_2H_6	0.063 ± 0.003	0.282 ± 0.029	0.55

and table 1 shows a summary of maximum drift field E/p values. Fig. 12 shows that the drifting electrons did not reach ionizing energies in the drift structure. Therefore the breakdown occurred somewhere on the imperfections of the stainless steel electrodes or the divider chain. Although the theory of breakdowns is more complicated [45,46,60,61], one clearly notices in case of the He-based gas mixtures a simple correlation between the breakdown voltage and size of the b constant in our data presented in table 1. The larger the b constant, the more readily can the electrons obtain large ionizing energies in a field of a sharp point.

From a practical point of view, when designing a large tracking chamber with many wires with for instance 95% He + 5% C_2H_6 gas, one may risk possible breakdown problems unless the field wires are appropriately large and without surface defects. For such applications we would recommend using at least 15–20% of some quenching gas to guarantee a reliable operation; in addition, one will have also much lower diffusion. However, under appropriate conditions, such as with good wire surfaces and low surface gradients, operation is possible with less quenching gas, as demonstrated by the PLUTO group which used the 93% He + 7% C_3H_8 gas with their large chamber [39].

One should also mention that in parallel plate chamber applications at normal pressure one finds it advantageous to have a gas such as 95% He + 5% C_2H_6 [38], because one achieves operating gains at lower operating voltages. But one must be careful designing the chamber near the edges and high voltage entry points to prevent the unwanted breakdowns.

3.6. Pulse height spectra, wire gain and poor quenching

The study of pulse height spectra initiated by single electrons is useful not only from the theoretical point of view, but also to reveal problems such as insufficient quenching. Such problems can cause very broad single electron pulse height spectra which, in turn, can worsen dE/dx resolution in the tracking chamber and cause afterpulsing, or even wire aging, since such behavior will increase the total wire charge dose. We have used the following parametrization of the Polya function [47–51] to fit our data:

$$P(q) \cong \left[(1+\theta)\frac{1}{\bar{q}}\right]^{\theta} e^{-(1+\theta)(q/\bar{q})}, \qquad (2)$$

where q = number of electrons in avalanche and $\bar{q}$ = mean number of electrons in avalanche.

One should stress that this equation is based on a theory which includes ionization by electron impact only; secondary processes taking place in the gas or at the cathode are neglected. When secondary processes become significant, multiple avalanches can occur [52,53]. An example of the physical origin of such secondary avalanches is photoeffect at the cathode. The close proximity of the nickel plated cathode to the sense wire in our geometry may help to enhance the multiple avalanche effect compared to a more open geometry.

The exact physical significance of the parameter θ is not clear. But if the parameter θ is zero the function becomes the Furry exponential law. One typically observes such exponential dependency at low E/p in the

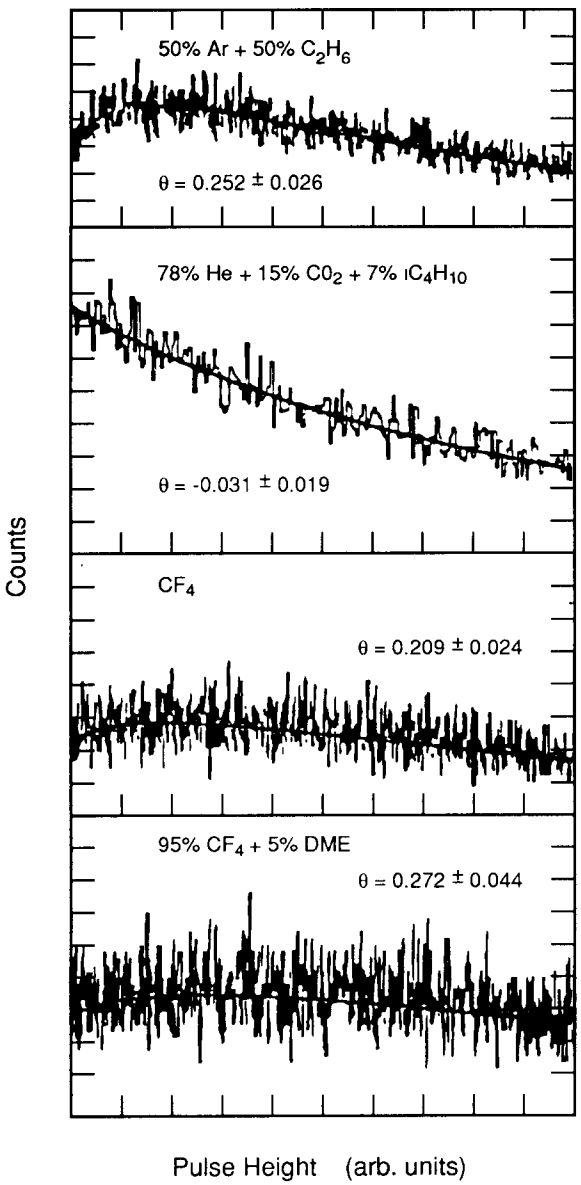

Fig. 13. Our measurement of the single electron pulse height spectra with Polya fits in various gases.

avalanche region, i.e., low wire gains. If θ is positive, one obtains a peaked distribution. Fig. 13 shows some examples of our measured single electron pulse height spectra for several gases. Table 2 shows the summary of the Polya fits, including the mean visible wire gain in various gases, surface field on the 20 μm diameter anode wire and χ^2/degree of freedom as a measure of quality of the fit. As we stated in section 2 the pulse height region near the pedestal (below 2–4 fC of signal charge) was not used in the fit.

One can also see that several He gas mixtures yield a negative θ. This behavior is connected with excessive tails in the pulse height distributions. Fig. 14a shows one such example from our data using 95% He + 5% C_2H_6 gas. The data were taken with the qVt gate width of about 450 ns to integrate multiple pulses.

It has been suggested by Legler [52] that such a tail may be associated with "avalanche breeding" (primary avalanche followed by secondary avalanches). Byrne et al. [53] have tested this theory in a tube detector operating with 90% Ar + 10% CH_4 gas at a low pressure of 80 mm Hg. Their E/p in the avalanche region was between 144 and 166 V/cm/Torr and the wire gain between 7×10^3 and 4.3×10^4. Fig. 14b clearly indicates that at larger E/p the pulse height spectrum develops an excessive tail. It was suggested that the amount of methane used was not sufficient to quench UV photons from the argon atoms entirely and a chain of avalanches developed.

Therefore we argue that also in our measurements of the He gases when we see negative θ, there is an insufficient amount of quenching. We have tested the gases having negative θ at as low gain as possible to try to reduce this effect to its minimum. Also, this effect

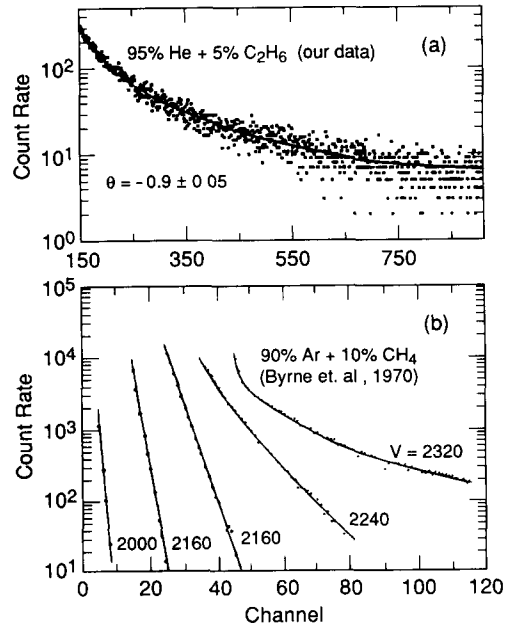

Fig. 14. (a) Our measurement of the single electron pulse height spectra in 95% He + 5% C_2H_6 gas. The negative θ is indicative of some avalanche breeding (see text). (b) Data of Byrne et al. [47] with single electron pulse height spectra as a function of counter voltage. At $V = 2320$ one sees a sign of avalanche breeding, i.e., poor quenching. The E/p range was 144–166 V/cm/Torr and the pressure was 80 mm Hg.

can be seen in the He + DME mixtures where we varied the mixing ratio. The θ changes from negative to positive as the amount of DME quencher is increased. Fig. 15 and table 2 show this dependence.

Table 2
Summary of Polya fits to single electron pulse heights

Gas	V_c [kV]	Approx. E_a [kV/cm]	Mean visible gain $\bar{q}$	θ	χ^2/n_D
50% Ar + 50% C_2H_6	−1.5	311	5.0×10^5	0.252 ± 0.026	1.05
95% CF_4 + 5% DME	−1.85	377	9.2×10^5	0.272 ± 0.044	1.04
80% CF_4 + 20% C_4H_{10}	−1.7	349	3.4×10^5	0.624 ± 0.043	1.15
90% CF_4 + 10% CH_4	−1.95	396	6.3×10^5	0.222 ± 0.042	1.18
100% CF_4	−1.95	396	7.5×10^5	0.209 ± 0.024	1.02
50% He + 50% C_2H_6	−1.45	302	2.9×10^5	0.287 ± 0.019	1.02
78% He + 15% CO_2 + 7% C_4H_{10}	−1.35	283	5.8×10^5	−0.031 ± 0.019	1.01
100% DME	−1.87	381	4.5×10^5	1.768 ± 0.079	0.96
80.5% He + 19.5% DME	−1.25	264	4.1×10^5	0.321 ± 0.058	1.06
86.5% He + 13.5% DME	−1.15	245	3.0×10^5	0.110 ± 0.025	1.01
92–9.% He + 7.1% DME	−1.0	216	1.3×10^5	−0.532 ± 0.05	1.18
96.4% He + 3.6% DME	−0.85	188	1.9×10^4	−0.897 ± 0.05	1.59
93% He + 7% C_3H_8	−0.97	211	1.1×10^5	0.537 ± 0.05	1.15
95% He + 5% C_2H_6	−0.85	188	2.6×10^4	−0.9 ± 0.05	1.25

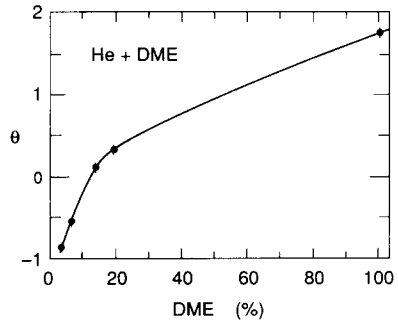

Fig. 15. Our data for θ fits (eq. (2)) for the He+DME mixtures. Negative θ indicates a poor quenching; the solid curve is to guide the eye.

One needs at least 12–15% of DME to quench the He gas according to this criteria. This correlates with the cathodic breakdowns we have reported earlier. Schmidt et al. [43] independently found that 10% of DME quencher in the He gas is not enough to prevent these secondary effects. The two other relatively better-quenched He-based gases, 50% He + 50% C_2H_6 and 78% He + 15% CO_2 + 7% iC_4H_{10}, have θ equal 0.287 $\pm$ 0.019 and -0.031 ± 0.019, respectively. One may argue that the amount of quencher in the second gas should not be reduced since θ is near zero. The CF_4 gas behaves well, but it does exhibit a distribution having negative θ if the wire gain is larger than about 10^6. It should be noted, that the fits with negative θ are generally of worse quality, indicating that eq. (2) is probably not the completely correct function to describe the underlying physical process of multiple avalanches. Nevertheless, we have found this parametrization quite useful in recognizing poor avalanche quenching.

3.7. Diffusion near the anode wire

Near anode wire diffusion has been discussed by Villa [3] in connection with DME and the question how to achieve the best possible tracking resolution. He has pointed out that since the characteristic electron energy increases as a function of electric field at least quadratically (see table 1), one could have a significant contribution due to the diffusion near the anode wire.

We will discuss two gases, 78% He + 15% CO_2 + 7% iC_4H_{10} and CF_4. The first gas was chosen because the He-based gases can become nonthermal more quickly. Is this an important factor in the final tracking resolution? Do we have to choose the operating point carefully to limit this contribution? The CF_4 gas was chosen because it is well known [54] that it absorbs electrons if they reach about 6–7 eV where the electron attachment cross section has a maximum. Would this show up in measured resolution at large wire gains because the avalanche charge fluctuates more (in addition to an effect of electron loss)?

Fig. 16a shows schematically our measurement of diffusion for various distances from the wire. The linear curve through our data points can be extrapolated

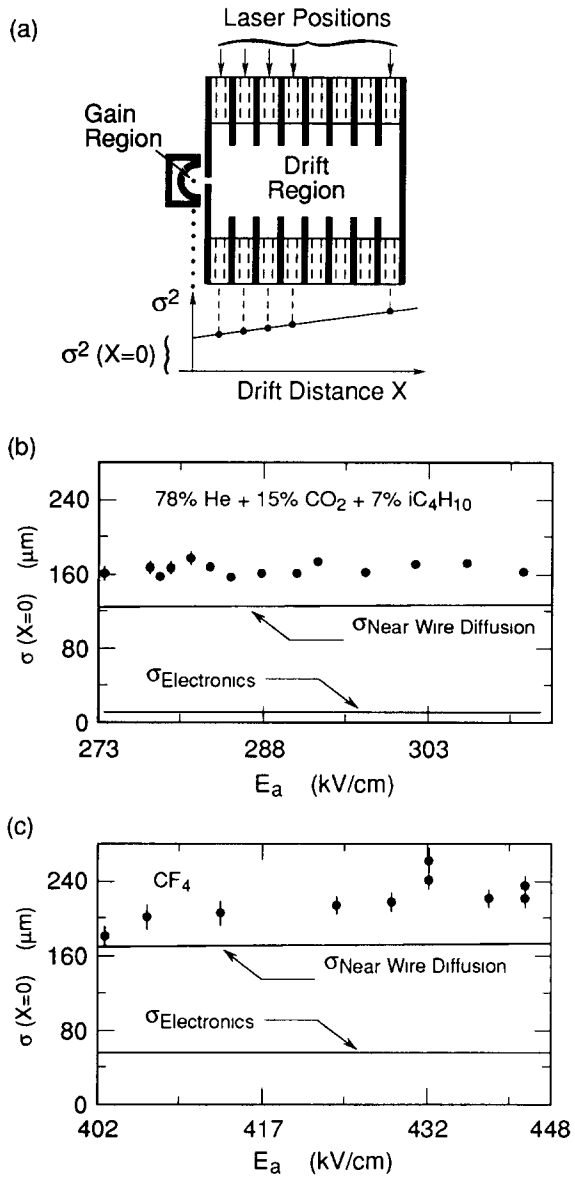

Fig. 16. (a) Schematic description of $\sigma(x = 0)$ as measured in the single electron longitudinal diffusion test. Our measurement of $\sigma(x = 0)$ dependence on the wire gain expressed in terms of the anode surface gradient E_a in (b) 78% He + 15% CO_2 + 7% iC_4H_{10} gas ($E_{drift} = 206$ V/cm), and (c) CF_4 gas ($E_{drift} = 102$ V/cm). The final offset $\sigma(x = 0)$ is the sum in quadrature of $\sigma_{\text{Laser induced spot size}}$, $\sigma_{\text{Electronics}}$ and $\sigma_{\text{Near Wire Diffusion}}$ (see text).

to the origin $x = 0$, i.e., the wire position, and we can predict an offset $\sigma^2(x = 0)$. Because we are dealing with single electrons only, there are three contributions to $\sigma(x = 0)$; namely a contribution due to the laser induced spot size, the electronics resolution and a contribution due to the near wire diffusion. The laser induced spot size was estimated to be less than 20 μm (σ). The electronic resolution contains mainly its slewing response to avalanche fluctuations. To estimate the electronics contribution we injected at the input of the amplifier charge pulses of different amplitudes representing a typical range of single electron pulse heights. From the observed time spread and the known drift velocity in the drift region one can then estimate the electronics contribution to $\sigma(x = 0)$ [figs. 16b and 16c]. We have chosen a low drift field (206 V/cm and 102 V/cm, respectively) in order that the drift velocity be small and resulting electronics contribution to the final error in $\sigma(x = 0)$ also be small. The laser induced spot size and the electronics contributions alone cannot explain the data and we need some additional effect to explain the size of $\sigma(x = 0)$. The near wire diffusion can explain the discrepancy as we will see in the following simple calculation.

To calculate the near wire diffusion we have used two methods. In the case of 78% He + 15% CO_2 + 7% iC_4H_{10} we used our measurement of characteristic energy as a function of electric field (table 1) and extrapolated it to very large fields near the wire. We stepped in $x = 10$ μm increments from the pin hole to the anode wire, and calculated a contribution to the single electron longitudinal dispersion at each step according to the formula:

$$\sigma_L = \sqrt{\frac{3\epsilon_L x}{E}} \,. \tag{3}$$

In case of CF_4, we used a known characteristic energy at very large fields as measured by Naidu and Prasad [36], and took the liberty to use their transverse characteristic energy with our longitudinal measurement (see fig. 17 for the polynomial fit used in the calculation). In this case, we stepped in $t = 100$ ps increments, and evaluated (4) in each step, using the diffusion coefficient D_L previously evaluated using eq. (1):

$$\sigma_L = \sqrt{2D_L t} \,. \tag{4}$$

Results of this analysis are shown in fig. 16b and 16c where we vary the gain on the wire while keeping the drift field constant at 206 V/cm/atm and 102 V/cm/atm, respectively. One can also see that the $\sigma(x = 0)$ does not vary over a practical range of gain variation, indicating that the near wire diffusion is not very sensitive to the gain setting. However it is interesting to see that the near wire diffusion may indeed dominate the single electron offset $\sigma(x = 0)$.

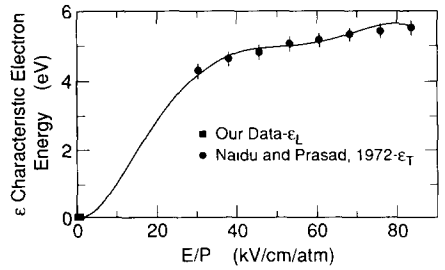

Fig. 17. Characteristic transverse electron energy data of Naidu [27] plotted together with our data of characteristic longitudinal electron energy. The curve is a polynomial fit.

If n primary electrons enter the avalanche, then the near wire diffusion contribution gets reduced by a factor of $\sqrt{n}$, provided that they arrive together within the resolution time. For large enough n and/or at large drift field, the electronics resolution will dominate $\sigma(x = 0)$. Therefore, in practice the near wire diffusion may be important only for applications where the ultimate resolution is wanted.

Clearly, the limitation of this analysis is the lack of exact knowledge of ϵ_L near the wire. In addition, we have not treated the problem as a three-dimensional Monte Carlo (possibly using the Biagi program output), but only as one-dimensional numerical calculation. This is, perhaps, why there is a small disagreement between the calculation and measurement.

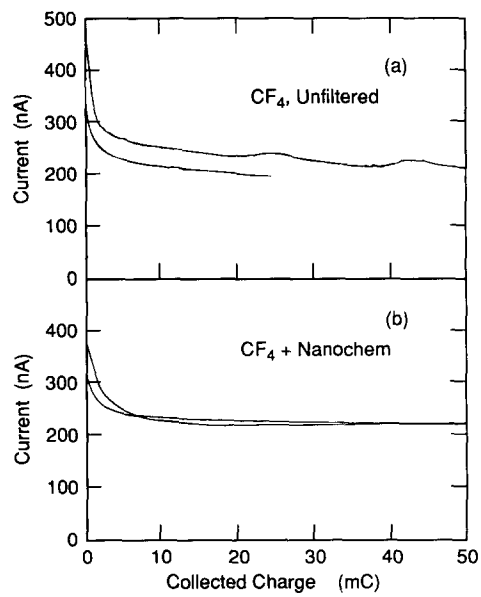

Fig. 18. Our measurements of the wire aging in CF_4 gas in the tube geometry. Approximately 3 mm of wire length was irradiated. (a) Without the Nanochem filter. (b) The same with the Nanochem filter.

3.8. Wire aging

The wire aging study was performed in an apparatus described previously [55]. For these tests we used copper tubes of about 1 cm diameter with a 50 μm diameter gold-plated tungsten sense wire.

Wire aging in CF_4-based gases has been discussed in more detail previously [1,2,56,57]. To our surprise, we observed a significant aging rate for pure CF_4 gas as one can see in fig. 18a. The wire gain drops by more than 100 000%/C/cm in the first few mC of a charge dose. This was not expected since we did measure very low aging rates with mixtures such as 80% CF_4 + 20% iC_4H_{10} [1,2,56]. We were therefore motivated to include the Nanochem filter to clean the gas, to see if the Nanochem filter had the same beneficial effect upon the wire aging as it has on the mean drift length (see section 3.2). As shown in fig. 18b, there was no significant improvement in the aging rate.

We selected two types of He-based gases for the wire aging, 95% He + 5% C_2H_6 in which the electrons heat up easily, and the second was 78% He + 15% CO_2 + 7% iC_4H_{10} which is better quenched. Fig. 19 shows the results. The wire aging rate in 95% He + 5% C_2H_6 gas is consistent with zero having a measured value of 0.1 ± 0.1%/C/cm. However, a moderate wire aging was observed in the gas 78% He + 15% CO_2 + 7% iC_4H_{10}, where we obtained 30 ± 0.2%/C/cm.

Why the CF_4 gas results in aging and the 80% CF_4 + 20% iC_4H_{10} gas does not, is not understood and indicates a lack of some knowledge of details of the avalanches. For example, the electron energy may be sufficiently different, with and without iC_4H_{10}, that the rate of polymerization processes is affected, or some chemistry involving the iC_4H_{10} may suppress the deposits which occur with pure CF_4.

The Biagi MAGBOLTZ [24] program seems to reproduce our data and it is believed to do a reasonable job at even higher electric fields [26]. We have decided to use it to try to predict the electron average energy as

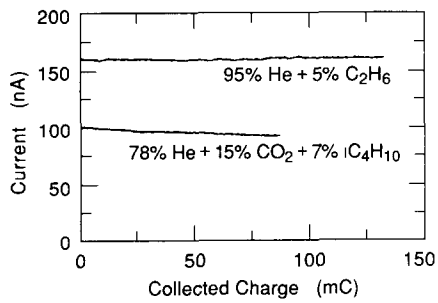

Fig. 19. Our measurement of the wire aging in 95% He + 5% C_2H_6 and in 78% He + 15% CO_2 + 7% iC_4H_{10} gases using the same geometry as for CF_4 tests (fig. 18).

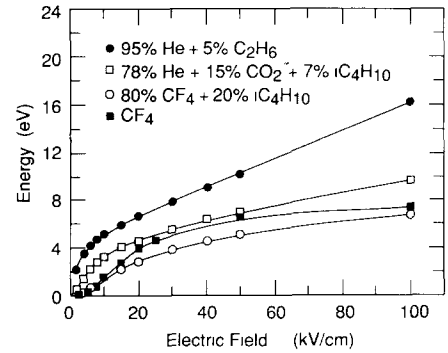

Fig. 20. Average electron energy as calculated using the Biagi's program [24] in gases we have used for the wire aging. Curves are eye guidance.

high as 100 kV/cm for all four types of gases used in our wire aging test. The aim was to quantify average electron energies very near the wire. The result of this calculation is shown in fig. 20. One can notice that the iC_4H_{10} component in the 80% CF_4 + 20% iC_4H_{10} mixture tend to cool down the electrons somewhat. On the other hand, the electrons in both He-based gases are hotter than for the CF_4-based gases.

It is well known that the CF_4 molecule can absorb an electron and dissociate to form F^- and CF_3^- negative ions together with F^*, CF_2^* and CF_3^* radicals. The probability for this process peaks at an electron energy of about 6–7 eV [34], i.e., the process occurs only very near the wire. The iC_4H_{10} admixture will tend to lower the average electron energy in the avalanche as one can see in fig. 20, and therefore it will reduce the probability of the negative ion formation. The negative ions will tend to drift towards the anode wire. It is presently unclear why this mechanism will produce a different rate of wire aging between the two above mentioned CF_4-based gases. One possibility is that in case of 80% CF_4 + 20% iC_4H_{10} the iso-butane serves as a material on which the fluorine and fluorocarbon radicals react and the resulting products tend to be volatile. This hypothesis was mentioned in connection to an ability of some CF_4 gas mixtures to etch away the previously created aging deposits [58]. Apparently, this mechanism is absent in case of CF_4 gas alone and the anode wire is coated, or its surface reacts to form a nonconducting metal fluoride [59].

On the other hand, the electrons in the 95% He + 5% C_2H_6 gas mixture tend to be much hotter, as one can see in fig. 20. Perhaps, they can destroy any polymerization product and resulting species are volatile.

More work in this area is needed to understand the process of wire aging. But it is of some interest to introduce the electron transport program into the wire aging problem to start quantifying some of the parameters involved.

4. Conclusions

To summarize our results:

(a) We have measured drift velocity and longitudinal single electron diffusion in CF_4 and He-based gases. Using this data, we have calculated the characteristic electron energy as a function of electric field. While CF_4 gases are nearly thermal up to at least 2 kV/cm/atm, the He mixtures show larger diffusion unless about 15–20% of quenching gas is used.

(b) Addition of 5% of DME to CF_4 slows it down considerably, more so than 20% of iC_4H_{10}.

(c) The CF_4-based gases are prone to contain impurities resulting in electron attachment. The use of a Nanochem filter can solve this problem.

(d) Wire aging in CF_4 gas without any additive is surprisingly fast. The Nanochem filter does not help in this case. We found negligible wire aging in the 95% He + 5% C_2H_6 mixture and only moderate aging in 78% He + 15% CO_2 + 7% iC_4H_{10}.

(e) We have measured single electron pulse height spectra and wire gains in the CF_4 and He-based gas mixtures. Some He-based mixtures with a small amount of quenching gas indicate the presence of excessive number of larger pulses in our geometry. This effect shows up as a negative θ variable in eq. (2).

(f) CF_4 alone quenches well in a single electron mode up to gains of about 10^6.

(g) We have studied the influence of water on the drift velocity and diffusion. The drift velocity changes by about 6.3% per 1000 ppm water addition at a drift field of 1.5 kV/cm/atm in 80% CF_4 + 20% iC_4H_{10} gas.

(h) The electrons in the He-based gases tend to be "hot" even at modest electric fields if the amount of quenching gas used is small, and this is also associated with lower cathodic breakdown voltages.

(i) The near wire diffusion is not very sensitive to the gain setting. However, it may indeed dominate the single electron offset $\sigma(x = 0)$ in some gases. It may be important only if one wants to achieve the ultimate tracking resolution, but in most practical cases, it is not a serious concern. We have not found a serious effect of near wire diffusion for CF_4 at high gains.

(j) We found an excellent agreement between our drift velocity and longitudinal diffusion data and the second-order solution to the Boltzmann equation of Biagi [24]. However, the predictions involving the CF_4 and DME gases are worse than those for other gases, probably due to inconsistencies in existing CF_4 and DME data.

(k) Among the gases we have studied in this paper, we would presently choose 80% CF_4 + 20% iC_4H_{10} as a fast gas candidate, and 50% He + 50% C_2H_6 or 80% He + 20% DME or 78% He + 15% CO_2 + 7% iC_4H_{10} as low mass gas candidates for the large tracking chambers. We would not reduce the amount of quencher in the last gas.

Acknowledgements

We would like to thank O. Millican and M. Neibel for help during various stages of this test. We thank to Dr. S. Biagi for providing his electron transport calculations for various gases in the paper. We also thank Drs. G. Viertel and H. Anderhub for running the WIRCHA program for us.

Note added in proof

In section 3.8 of this paper, we stated that a rapid decrease in anode current is observed in accelerated aging tests with CF_4. In addition, we postulated chemical effects that may cause this aging and explain why the presence of iC_4H_{10} in CF_4/iC_4H_{10} (80/20) eliminates the aging.

As a result of further experimentation, we believe that the rapid decrease in current observed in CF_4 may not reflect anode aging. Indeed, we have used CF_4 to etch anode deposits. To explain the aging properties of CF_4/iC_4H_{10} gas mixtures, we have developed a four-part model considering: 1) plasma polymerization of the hydrocarbon, 2) etching of wire deposits by CF_4, 3) acceleration of deposition processes in strongly etching environments, and 4) reactivity of the wire surface. Details of this model and aging results in CF_4/iC_4H_{10} gases are presented elsewhere [59].

References

[1] R. Kotthaus (p. 161), A. Wagner et al. (pp. 195, 327), H. Kado (p. 207), D. Binnie (pp. 213, 311) and H. Sadrozinski (p. 121), Proc. Workshop on Radiation Damage to Wire Chambers, Lawrence Berkeley Laboratory, Berkeley, CA 94720, USA, ed. J. Kadyk, LBL, LBL-21170 (1986).
J.A. Kadyk, Nucl. Instr. and Meth. A300 (1991) 436;
J. Va'vra, Nucl. Instr. and Meth. A252 (1986) 547; and SLAC-PUB-5207 (1990).
[2] J. Kadyk, J. Va'vra and J. Wise, Nucl. Instr. and Meth. A300 (1991) 511.
[3] F. Villa, Nucl. Instr. and Meth. 217 (1983) 273.
[4] LSI Laser Science Model VSL-337ND,
[5] Oriel Model 18512, Stratford, CT 06497-0872, USA.
[6] EG&G Model FND-100, Salem, MA 01970-0662, USA.
[7] J. Va'vra et al., SLAC-PUB-4432 (September 1987).
[8] P. Antilogus et al., SLAC-PUB-5120 (October 1990).
[9] Y. Fukushima et al., Nucl. Instr. and Meth. A283 (1989) 709.
[10] H. Van Der Graff and H. d'Achard Van Enschut, Nucl. Instr. and Meth. A241 (1985) 387.

[11] Keithley digital meter 196 with Keithley digital scanner 705, Keithley Instruments, Inc., Cleveland, OH 44139, USA.
[12] Thermistor YSI 44201, Yellow Springs, OH 45387, USA.
[13] Setra Model 270, Acton, MA 01720, USA.
[14] Teledyne Model 316RAX, City of Industry, CA 91749-1580, USA.
[15] Panametrics Model 3A, Waltham, MA 02154-3497, USA.
[16] S. Cittolin et al., CERN-UA1 TN 90-01.
[17] Datametrix Model 825, Edwards High Vacuum, Grand Island, NY 14072, USA.
[18] A.E. O'Keeffe and G.C. Ortman, Anal. Chem., 38 (1966) 760; and 41 (1969) 1598.
[19] A. Peisert and F. Sauli, CERN 84-08.
[20] L. Wong, J. Armitage and J. Waterhouse, Nucl. Instr. and Meth. A273 (1988) 476.
[21] J. Fehlmann, P. Hawelka, D. Linnhoefer, J. Paradiso and G. Viertel, ETH Zurich Internal Report (1983).
[22] B. Jean-Marie, V. Lepeltier and D. L'Hote, Nucl. Instr. and Meth. 159 (1979) 213.
[23] F. Piuz, Nucl. Instr. and Meth. 205 (1983) 425.
[24] S. Biagi, Nucl. Instr. and Meth. A283 (1989) 716.
[25] Private communications from M. Yousfi, Centre de Physique Atomique, Universite Paul Sabatier, Toulouse, France.
[26] S.F. Biagi and P.S.L. Booth, Nucl. Instr. and Meth. A273 (1988) 530.
[27] G.W. Fraser and E. Mathieson, Nucl. Instr. and Meth. A257 (1987) 339.
[28] J. Fehlmann, J. Paradiso and G. Viertel, WIRCHA Simulation program, ETH Zurich (March 1983) and J. Fehlmann, Ph.D. thesis No. 8711, ETH Zurich (1988).
[29] L.G.H. Huxley and R.W. Crompton, The Diffusion and Drift of Electrons in Gases (Wiley, New York, 1974).
[30] Matheson Gas Co., Newark, CA 94560, USA.
[31] Nanochem Model L-60, Semi-gas System Inc., San Jose, CA 95126, USA.
[32] A special production of DME gas delivered to S. Majewski from DuPont Chem. Co.
[33] B. Schmidt and S. Polenz, Nucl. Instr. and Meth. A273 (1988) 488.
[34] L.G. Christophorou et al., Nucl. Instr. and Meth. 163 (1979) 141.
[35] S.R. Hunter, J.G. Carter and L.G. Christophorou, J. Appl. Phys. 58 (1985) 3001.
[36] M.S. Naidu and A.N. Prasad, J. Phys. D: Appl. Phys., 5 (1972) 983.
[37] S.M. Playfer et al., ETHZ-IMP-PR-91-3 (1991).
[38] N. Solomey et al., Nucl. Instr. and Meth. A283 (1989) 673
[39] W. Zimmermann et al., Nucl. Instr. and Meth. A243 (1986) 86.
[40] M. Basile et al., CERN-EP/85-40 (March 1985).
[41] T.L. Cottrell, W.J. Pollock and I.C. Walker, Trans. Faraday Soc. (1968).
[42] P.R. Burchat, J. Hiser, A. Boyarski and D. Briggs, SLAC-PUB-5626 (1991); this gas mixture was suggested by A. Seiden and was used in the Mark II group tests as a part of R&D for the B Factory.
[43] B. Schmidt and K. Martens, HD-PY 92/01.
[44] L.S. Frost and A.V. Phelps, Phys. Rev. 127 (1962) 1621.
[45] H. Raether, Z. Phys. 112 (1939) 464.
[46] J.M. Meek, Phys. Rev. 57 (1940) 722.
[47] J. Byrne, Proc. Roy. Soc. Edinburgh 66A (1962) 33.
[48] L. Lansiart and J.P. Morucci, J. Phys. Rad. Suppl., No. 6, 23 (1962) A102.
[49] A.H. Cookson and T.J. Lewis, Brit. J. Appl. Phys. 17 (1966) 1473.
[50] G.D. Alkhazov, Nucl. Instr. and Meth. 89 (1970) 155.
[51] H. Genz, Nucl. Instr. and Meth. 112 (1973) 83.
[52] W. Legler, Z. Naturforsch. 19a (1964) 481.
[53] J. Byrne, F. Shaikh and J. Kyles, Nucl. Instr. and Meth. 79 (1970) 286.
[54] S.R. Hunter and L.G. Christophorou, J. Chem. Phys. 80 (1984) 6150.
[55] J Kadyk and J. Wise, IEEE Trans. Nucl. Sci. NS-37 (1990) p. 478;
and J. Wise, M.S. thesis, LBL-29033 (1990).
[56] R. Henderson et al., IEEE Trans. Nucl. Sci. NS-34 (1987) p. 528.
[57] B. Dolgoshein et al., CERN-EP/89-161.
[58] R. Openshaw et al., Nucl. Instr. and Meth. A307 (1991) 298.
Also, see J.A. Kadyk, Nucl. Instr. and Meth. A300 (1991) 454 (fig. 4).
[59] J. Wise, Ph.D. thesis, LBL-32500 (1992).
[60] F. Fonte, V. Peskov and F. Sauli, Nucl. Instr. and Meth. A305 (1991) 91.
[61] J. Va'vra, SLAC-PUB-5793 (1992).